STAR Protocols

CellPress
OPEN ACCESS

Protocol

Concurrent recordings of hippocampal neuronal spikes and prefrontal synaptic inputs from an awake rat

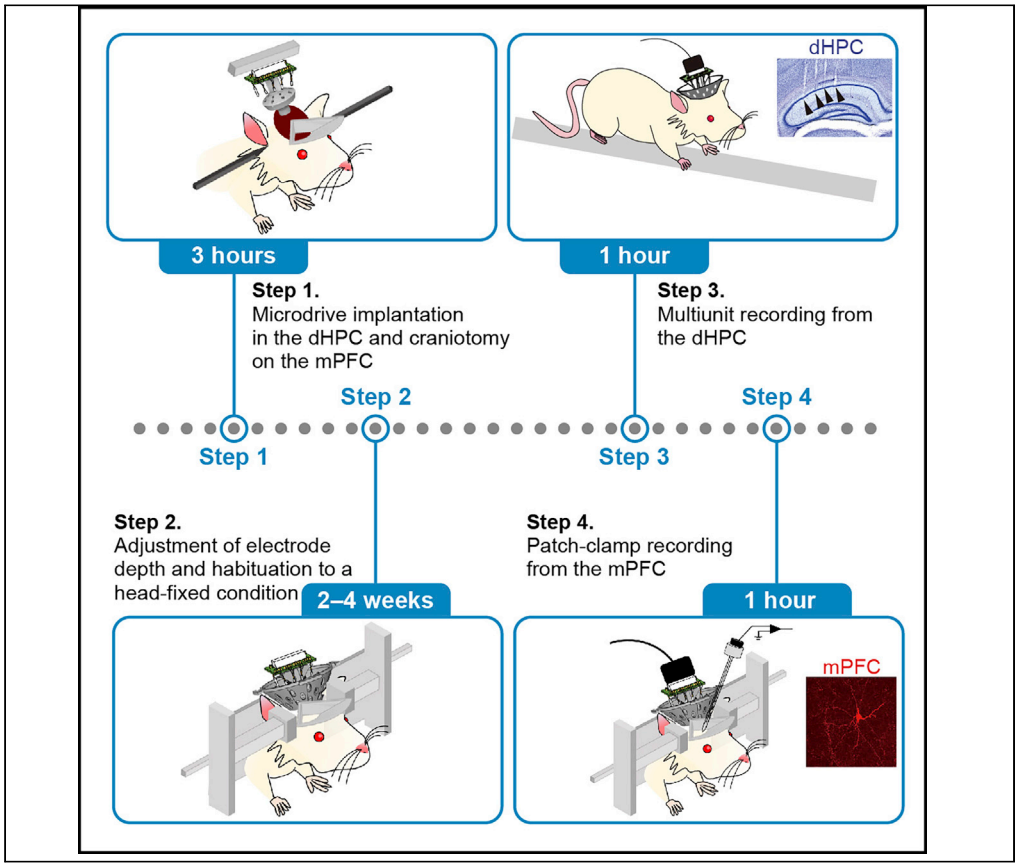

A major challenge in neuroscience is linking synapses to cognition and behavior. Here, we developed an experimental technique to concurrently conduct a whole-cell recording of a prefrontal neuron and a multiunit recording of hippocampal neurons from an awake rat. This protocol includes surgical steps to establish a cranial window and 3D printer-based devices to hold the rat. The data sets allow us to directly compare how subthreshold synaptic transmission is associated with suprathreshold spike patterns of neuronal ensembles.

Yuya Nishimura, Yuji Ikegaya, Takuya Sasaki

tsasaki@mol.f.u-tokyo.ac.jp

Highlights

A surgical craniotomy is performed on the prefrontal cortex

A microdrive is implanted on the hippocampus

A patch-clamp recording is obtained from a prefrontal neuron

Protocol allows simultaneous multiunit and whole-cell recordings

Nishimura et al., STAR Protocols 2, 100572
June 18, 2021
https://doi.org/10.1016/j.xpro.2021.100572

STAR Protocols

CellPress
OPEN ACCESS

Protocol

Concurrent recordings of hippocampal neuronal spikes and prefrontal synaptic inputs from an awake rat

Yuya Nishimura,[1] Yuji Ikegaya,[1,2,3] and Takuya Sasaki[1,4,5,6,*]

[1]Graduate School of Pharmaceutical Sciences, The University of Tokyo, 7-3-1 Hongo, Bunkyo-ku, Tokyo 113-0033, Japan

[2]Center for Information and Neural Networks, National Institute of Information and Communications Technology, 1-4 Yamadaoka, Suita City, Osaka 565-0871, Japan

[3]Institute for AI and Beyond, The University of Tokyo, Tokyo 113-0033, Japan

[4]Precursory Research for Embryonic Science and Technology (PRESTO), Japan Science and Technology Agency (JST), 4-1-8 Honcho, Kawaguchi, Saitama 332-0012, Japan

[5]Lead contact

[6]Technical contact

*Correspondence: tsasaki@mol.f.u-tokyo.ac.jp
https://doi.org/10.1016/j.xpro.2021.100572

SUMMARY

A major challenge in neuroscience is linking synapses to cognition and behavior. Here, we developed an experimental technique to concurrently conduct a whole-cell recording of a prefrontal neuron and a multiunit recording of hippocampal neurons from an awake rat. This protocol includes surgical steps to establish a cranial window and 3D printer-based devices to hold the rat. The data sets allow us to directly compare how subthreshold synaptic transmission is associated with suprathreshold spike patterns of neuronal ensembles.

For complete details on the use and execution of this protocol, please refer to Nishimura et al. (2021).

BEFORE YOU BEGIN

Brain functions are manifested through coordinated interplays of myriad neuronal spikes and synaptic transmission across neurons. Recent advancements in neurophysiological techniques to monitor and manipulate spike patterns of neuronal populations, such as multiunit recording, optical imaging, and optogenetic tools, have revealed detailed neuronal circuit dynamics that underlie a variety of animal behaviors and cognitive functions. However, there is little evidence for detailed intracellular and synaptic mechanisms at subthreshold levels that trigger and support spike patterns at suprathreshold levels in living animals. This issue can be examined by utilizing *in vivo* patch-clamp recording, a method that can directly measure subthreshold membrane voltage from a single neuron in living animals (Bittner et al., 2015; Ebbesen et al., 2017; Epsztein et al., 2010; Harvey et al., 2009; Inagaki et al., 2019; Lee et al., 2012; Margrie et al., 2003; Nelson et al., 1994; Pei et al., 1991; Poulet and Petersen, 2008).

Here, we developed an experimental technique by integrating an *in vivo* patch-clamp recording into multiunit recordings, enabling concurrent spike recordings of dorsal hippocampal (dHPC) neuronal ensembles and whole-cell recordings of medial prefrontal (mPFC) neurons in awake rats (Figure 1A).

Multiunit recording techniques have been widely utilized to record the spike patterns of neuronal ensembles, such as dHPC place cells, from freely moving animals. In conventional methods, a microdrive that accommodates movable tetrodes is fixed to the animal's head by putting adhesives or dental cement on all areas of the exposed skull. In these experiments, an additional experimental apparatus (e.g., patch-clamp pipettes) could no longer access the brain surface once a microdrive

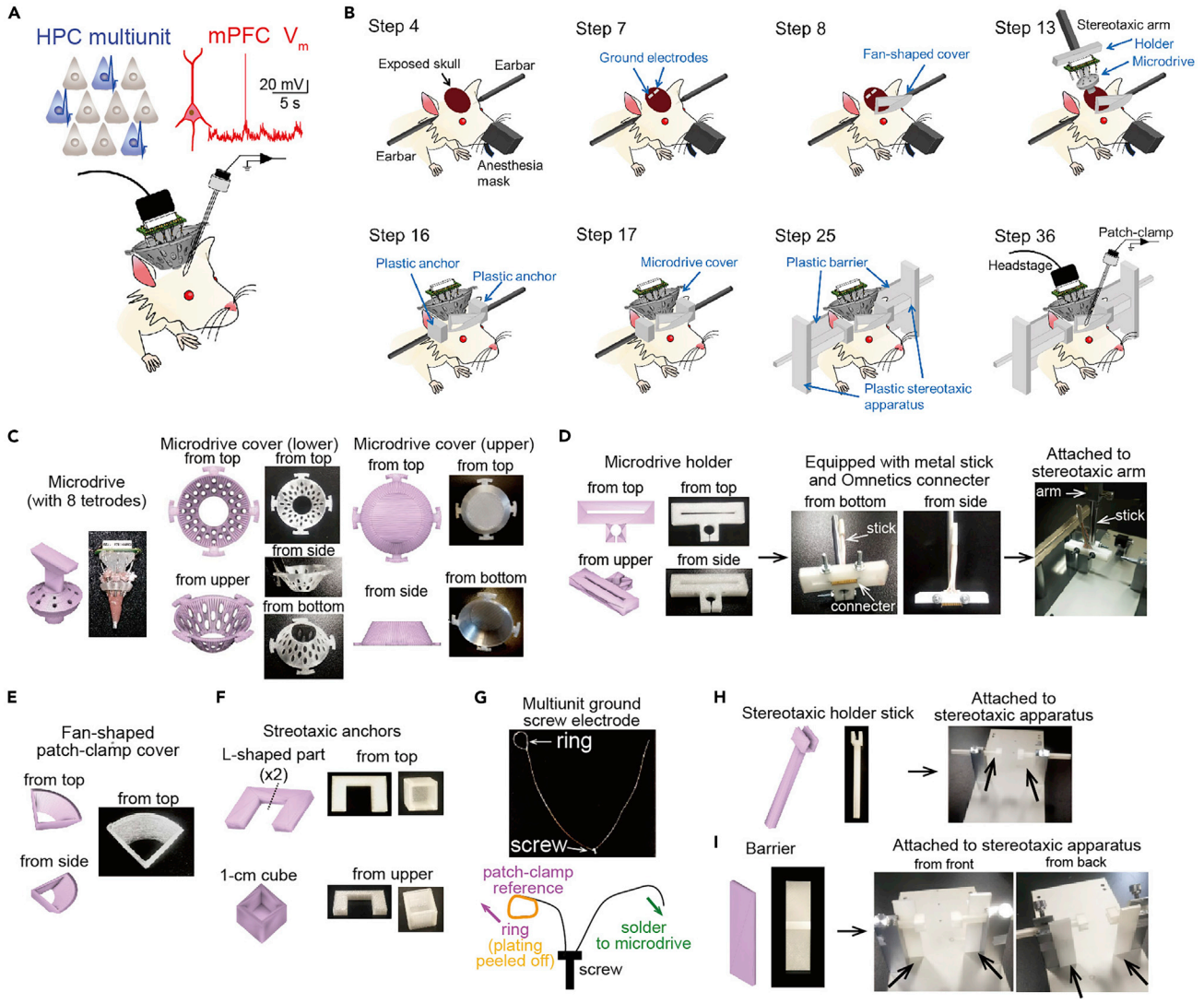

Figure 1. Custom-made materials

(A) A schematic illustration of recordings.

(B) Schematic illustrations of crucial steps and custom-made materials (blue) shown in C-I.

(C) CAD illustrations (pink) and the corresponding pictures of a microdrive and lower and upper parts of a microdrive cover.

(D) Microdrive holder. The holder accommodates an Omnetics connector in a rectangular hole and a metal stick in a circular hole. The stick is attached to a stereotaxic apparatus.

(E) Fan-shaped cover.

(F) Stereotaxic anchors for attaching to both sides of the ears of a rat. Two L-shaped parts are created by cutting the U-shaped part into two exact halves (dotted line).

(G) Microdrive ground screw electrode (top, picture; bottom, schematic illustration). The plating of the patch-clamp reference ring part is peeled off (orange).

(H) Stereotaxic holder stick. (Right panels) Two holder sticks from both sides through stereotaxic anchors to fix the rat (arrows).

(I) Barrier. (Right panels) Two barriers from both sides attached to the apparatus to prevent scratching by the hindlimbs.

was implanted. To resolve this technical issue, we developed an experimental protocol to implant a microdrive into the dHPC in rats without preventing patch-clamp recordings from mPFC neurons after implantation of the Microdrive (Nishimura et al., 2021). This protocol included several surgical steps that establish a cranial window on the mPFC; the use of custom-made parts, such as a cover and a stereotaxic apparatus, created by a 3D printer; and several histological confirmation steps from the two regions.

This method can be adapted for wider applications. First, this method is applicable to other brain region pairs with a distance of >5 mm apart on the horizontal plane of the brain surface (e.g., posterior parts of the brain (e.g., entorhinal cortex and cerebellum) for multiunit recordings and to anterior parts of the forebrain for patch-clamp recordings (e.g., motor cortex and piriform cortex [Davison and Ehlers, 2011; Inagaki et al., 2019; Poo and Isaacson, 2011]). Second, this patch-clamp recording can be implemented while rats engage in task paradigms, such as a lever press task, under head-fixed conditions. Third, a technique to create a craniotomy on the mPFC while keeping track of identical dHPC neuronal ensembles by multiunit recording may be combined with other recording and manipulation techniques, such as fiber photometry, optical imaging, microdialysis, local drug injection, and optogenetic photostimulation, instead of patch-clamp recordings. Fourth, a technique to implant a microdrive on the dHPC while maintaining a craniotomy for mPFC patch-clamp recordings may be combined with the implantation of other recording and manipulation apparatuses, such as cannula and optic fibers, instead of a microdrive. Before performing this protocol, one needs to be trained on standard procedures for multiunit recordings and patch-clamp recordings from living rodent animals. The details of these methods are described elsewhere (Lee et al., 2009; Lee et al., 2014; Petersen, 2017).

Animals

This protocol may be used for testing commercially obtained rats (e.g., purchased from the Jackson Laboratory) or transgenic rat lines newly created by research laboratories. Rats are maintained on a 12 h dark (7:00 AM–7:00 PM)/light (7:00 PM–7:00 AM) cycle so that all behavioral experiments occur in the dark phase.

> ***Note:*** All experiments must receive approval from the relevant institutional review board and be conducted according to the NIH guidelines for the care and use of rats. We obtained permission from the Experimental Rat Ethics Committee at the University of Tokyo (approval number: A30-72) to undertake the studies shown here.

> ***Note:*** If food restriction for rats is necessary for behavioral tests, the rats need to be housed individually before all experiments. Care must be taken to maintain their body weight at more than 85% of their ad libitum weight.

> ***Note:*** This protocol is reliably applicable to young male rats (3–5 weeks old) with a weight of less than 100 g throughout all experimental periods. The reasons to use young rats are that (1) younger rats generally yield recordings with lower series resistance in whole-cell recordings and (2) some larger rats (>100 g) move strongly during head fixation and destroy recording equipment, especially for plastic parts.

Custom-made plastic parts by a 3D printer

All the CAD files used in this paper are available at https://data.mendeley.com/datasets/4szrgxvm37/1.

The materials for creating the custom-made parts can be either ABS or PLA, thermoplastics insoluble in water. Before surgery, sterilize all of these parts with 70% ethanol.

1. Custom-made microdrive cover (Figure 1C)
   The microdrive cover is 37 mm in diameter and 13 mm in height (Figure 1C), created by a 3D printer. To reduce its weight, make 36 elliptical holes 4 mm in the major axis and 2 mm in the minor axis. The CAD file is available.
2. Custom-made microdrive holder (Figure 1D)
   The microdrive holder consists of a plastic part (40 mm × 21.5 mm in size and 4.7 mm in height) created by a 3D printer, an Omnetics connector (Omnetics Connector Corporation,

A79029-001), and a metal stick to attach to the stereotaxic arm (Figure 1D). This part is reusable. The CAD file is available.

3. Custom-made fan-shaped cover (Figure 1E)
   The fan-shaped cover is 14 mm in radius and 3.5 mm in height, created by a 3D printer. The CAD file is available.
4. Custom-made anchors for head fixation (Figure 1F)
   The anchor is composed of a 1-cm plastic cube and an L-shaped part (19.3 mm × 16.5 mm) for each side of the animal, created by a 3D printer. The CAD files are available.
5. Custom-made stereotaxic holder stick (Figure 1H)
   The stereotaxic holder stick is 80 mm in length, created by a 3D printer. These sticks are specific to the stereotaxic apparatus made by Narishige (e.g. SR-AR). These parts are reusable. The CAD files are available.
6. Custom-made barrier for stable head fixation (Figure 1I)
   The barrier is 70 mm × 19.6 mm in size, created by a 3D printer. These parts are reusable. The CAD files are available.

Microdrive

Make a microdrive accommodating 8 tetrodes (Figure 1C), including parts for assembling a microdrive (e.g., stainless-steel tubing, polyimide tubing, a plastic base created by a 3D printer, an electrical interface board, and tetrodes constructed from 17-μm-wide polyimide-coated platinum-iridium (90/10%) wire. More details have been described in previous papers (Jog et al., 2002; Kloosterman et al., 2009; Nguyen et al., 2009). The CAD files for making our microdrive are available. Set the tetrode tips with platinum and lower electrode impedances to 180–300 kΩ at 1 kHz. Leave the ground channels on the electrical interface board open.

Microdrive ground screw electrodes

For one rat, prepare two ground screw electrodes for multiunit recordings, termed multiunit ground screw electrodes. To make one multiunit ground screw electrode, cut a 7.0-cm piece of copper wire and solder one end to the head of a stainless-steel screw. In addition, cut a 10.0-cm piece of copper wire, form a wire ring with a diameter of ~1.0 cm by bending the wire, and fix the shape by soldering. Peel off the plating of the entire ring part. Solder the open end of the wire piece to the head of the stainless-steel screw. This ring serves as a reference electrode to connect to a patch-clamp recording system, termed a patch-clamp reference ring (Figure 1G).

Glass pipette electrodes

Pull glass pipettes with a resistance of approximately 4.0–7.0 MOhm. Ten to twenty pipettes must be prepared because a new pipette must be used for each attempt at patch-clamp recording.

KEY RESOURCES TABLE

REAGENT or RESOURCE	SOURCE	IDENTIFIER
Chemicals, peptides, and recombinant proteins		
Isoflurane	Pfizer	N/A
2% Lidocaine hydrochloride	AstraZeneca	e.g., Xylocain
10% Povidone-iodine	Avrio Health	e.g., Betadine
Sodium alginate	Sigma-Aldrich	cat. no. W201502
$CaCl_2$	Sigma-Aldrich	cat. no. 449709
Dental cement	Yamahachi Dental	Re-fine bright
Eye ointment	Allergan	Refresh Lacri-lube
Adhesive	Henkel	LOCTITE 454

(*Continued on next page*)

Continued

REAGENT or RESOURCE	SOURCE	IDENTIFIER
Adhesive accelerator	Henkel	LOCTITE SF7109
Chocolate milk	e.g., Meiji	N/A
K-gluconate	Sigma-Aldrich	cat. no. 60245
HEPES	Sigma-Aldrich	cat. no. H4034
Na_2-phosphocreatine	Sigma-Aldrich	cat. no. P7936
KCl	Sigma-Aldrich	cat. no. 60129
MgATP	Sigma-Aldrich	cat. no. A9187
Na_3GTP	Sigma-Aldrich	cat. no. G8877
EGTA	Sigma-Aldrich	cat. no. E3889
KOH solution	Merck KGaA	cat. no. 109108
Biocytin	Sigma-Aldrich	cat. no. B4261
KOH	Nacalai Tesque	28616-45
Urethane	Sigma-Aldrich	cat. no. U2500
Paraformaldehyde (PFA)	Nacalai Tesque	02890-45
Phosphate-buffered saline (PBS)	Takara Bio	T9181
Triton X-100	Sigma-Aldrich	cat. no. T8787
Sucrose	Nacalai Tesque	30403-55
Cresyl violet acetate	Sigma-Aldrich	C5042
Streptavidin, Alexa Fluor 594 Conjugate	Thermo Fisher Scientific	S11227
NeuroTrace 435/455 Blue Fluorescent Nissl Stain	Thermo Fisher Scientific	N21479
Experimental models: Organisms/strains		
Wistar/ST rat	SLC	N/A
Deposited data		
CAD files	This paper	https://data.mendeley.com/datasets/4szrgxvm37/1
Data sets	Nishimura et al., 2021	https://doi.org/10.17632/kc49ctr6yb.1
Other		
Polyurethane enameled copper wire (diameter: 0.14 mm, length 20 m)*	Oyaide	UEW
Polyimide tubing (outer diameter: 1.52 mm, inner diameter: 1.40 mm)*	Furukawa Sangyo	PIT-FS
Surgical tools (e.g., scissors, forceps, and spatula)	Fine Science Tools	N/A
Stainless steel screws (stem width: 1.4 mm, stem length: 3 mm)	MonotaRO	M1.4×3.0
26-gauge needles	Terumo	N/A
30-gauge needles	Misawa Medical Industry	No. 30
10-ml Syringe pressurizer	Terumo	1-4908-04
Alligator clip	N/A	N/A
Borosilicate glass capillaries (outer diameter: 1.5 mm, inner diameter: 0.84 mm)	World Precision Instruments	1B150F-4
Patch pipette fillers with a solution filter (diameter: 4 mm, 0.45-mm pores)	Millipore	Millex-LH
3D printer	Formlabs	Form 2
Inhalation anesthesia apparatus	Bio Machinery	TK-7
Stereomicroscope	Olympus	SZ2-STU3
Stereotaxic apparatus	Narishige	SR-6R-HT
Heating pad	Muromachi Kikai	FHC-HPS
Manipulator	Narishige	SMM-200
High-speed drill system	Narishige	SD-102
Digitally programmable amplifier	Blackrock	Cereplex M
Multiunit recording system	Blackrock	Cereplex Direct
Lightweight multiwire tether	Blackrock	BR9737
Video camera	Gazo	MCM-303NIR
Pipette puller	Sutter Instrument	P-1000

(*Continued on next page*)

Continued

REAGENT or RESOURCE	SOURCE	IDENTIFIER
Microforge	Narishige	MF-830
Vibration isolation table	Physio-Tech	M-86
Motorized stereotaxic-mounted Z micromanipulator	Narishige	DMX-1I
Patch-clamp amplifier, headstage, and ground electrode	Molecular Devices	MultiClamp 700B
Analog-to-digital converter	Molecular Devices	Axon Digidata 1550B
Vibratome	Dosaka	DTK-1000
Microtome	Leica	SM2010

*Parts for microdirve

MATERIALS AND EQUIPMENT

Name	Reagent	Amount
Sodium alginate solution	0.5% sodium alginate in saline. The solution can be stored at −20°C for three months.	1 mL
$CaCl_2$ solution	10% $CaCl_2$ in saline. The solution can be stored at −20°C for three months.	1 mL
Intracellular recording solution	135 mM K-gluconate, 10 mM HEPES, 10 mM Na_2-phosphocreatine, 4 mM KCl, 4 mM MgATP, 0.3 mM Na_3GTP (pH adjusted to 7.3 with KOH, target osmolality 285–289 mOsm), and 0.2% (wt/vol) biocytin. . The solution can be stored at −20°C for three months.	1 mL
Urethane solution	Make 0.1 g/ml urethane dissolved in saline. The solution can be stored at room temperature (23°C) for three months.	1 mL
Lidocaine solution	Make 0.5% lidocaine by diluting 2% lidocaine 4 times in saline. The solution can be stored at −20°C for three months.	1 mL
Triton X-100 solution	Make 0.2% Triton X-100 by diluting 20% Triton X-100 100 times in PBS. The solution can be stored at room temperature (23°C) for three months.	1 mL
NeuroTrace 435/455 blue fluorescent Nissl Stain solution	Make 0.4% NeuroTrace 435/455 blue fluorescent Nissl Stain by diluting NeuroTrace 435/455 blue fluorescent Nissl Stain 250 times in PBS	1 mL

Intracellular recording solution (Store at −20°C for three months)

Reagent	Final concentration	Amount
K-gluconate	135 mM	3.16 g
HEPES	10 mM	0.24 g
Na_2-phosphocreatine	10 mM	0.26 g
KCl	4 mM	0.030 g
MgATP	4 mM	0.20 g
Na_3GTP	0.3 mM	0.016 g
biocytin	0.2% (wt/vol)	0.2 g
ddH_2O	N/A	~100 mL
Total	N/A	100 mL

Adjust the pH of the solution with KOH to 7.2–7.3 and check osmolarity of the solution. For patch clamping, 280–290 mOsm/L is good. Keep the solution on ice throughout the experiment.

An alternative equipment: The equipment stated above are exmample electrophysiological recording setups. Multiunit recording setups are available from the other vendors such as Neuralynx and Intan technologies. Patch-clamp recording setups are available from the other vendors such as HEKA and Sutter Instrument. A stereotaxic appratus is avilable from the other vendors such as Kopf.

STEP-BY-STEP METHOD DETAILS

Surgery

Timing: 3 h

A Microdrive is implanted above the dHPC and a craniotomy is created on the skull above the mPFC for patch-clamp recordings.

1. Anesthetize the rat by inhalation of isoflurane gas at a concentration of 3.0% using standard methods.

⚠ CRITICAL: Appropriate regulations and guidelines for rat experiments must be followed.

⚠ CRITICAL: Lower the concentration of isoflurane gas to 1%–2% 15 min after the start of anesthesia. Monitor the animal's respiration rates throughout the anesthesia period.

2. Place the rat on a heating pad, shave the fur from the top of the head and then fix the head in the stereotaxic instrument with two ear bars and a nose clamp.
3. Inject 0.03 ml of 0.5% lidocaine as a local anesthetic into the scalp (s.c.), apply eye ointment, and then cover the eyes with aluminum foil to protect them from the surgical light. Clean the surface of the head skin with betadine.
4. Make an incision along the midline of the scalp from the area between the eyes to the back of the head and remove the periosteal soft tissue within the incised area. Clean the surface of the skull.

⚠ CRITICAL: Confirm that the height of the bregma and the lambda are similar horizontally.

5. Mark the target positions of the centers of the craniotomies with a black pen (3.0 mm anterior and 1.2 mm lateral to bregma for the right mPFC; 3.6 mm posterior and 4.0 mm lateral to bregma for the right dHPC).
6. Make 13 holes (0.8 mm diameter) in the skull at areas indicated by black dots in Figure 2A (their coordinates described in Figure 2A), using a high-speed drill (Figure 2B_1). Implant a stainless-steel screw into each of the holes as an anchor.

⚠ CRITICAL: The sites of the stainless-steel screws must be more than 3 mm distant from the two craniotomy centers.

⚠ CRITICAL: The screws on the frontal side are especially crucial, as they serve as anchors to attach to the fan-shaped cover with adhesive at step 8.

7. Using a high-speed drill, make 2 holes (0.8 mm diameter) in the skull above the cerebellum (6.0 mm posterior and 2.0 mm bilateral to bregma) (Figure 2B_2), as shown by cyan dots in Figure 2A, and implant a multiunit ground screw electrode into each of the holes.
8. Place the hole of the fan-shaped cover around the craniotomy and attach to the skull with adhesive (Figure 2B_3). Put a small drop of adhesive accelerator to facilitate the effect of the adhesive. This cover is necessary to protect against invasion of dental cement and serve as a saline storage pool for placing a patch-clamp ground electrode for subsequent patch-clamp recordings.

⚠ CRITICAL: The positioning of the fan-shaped cover is crucial. The distance between the posterior end of the fan-shaped cover and the anterior end of the craniotomy for the dHPC must be more than 3.0 mm. If this distance is too short, the patch-clamp pipettes physically interfere with the microdrive.

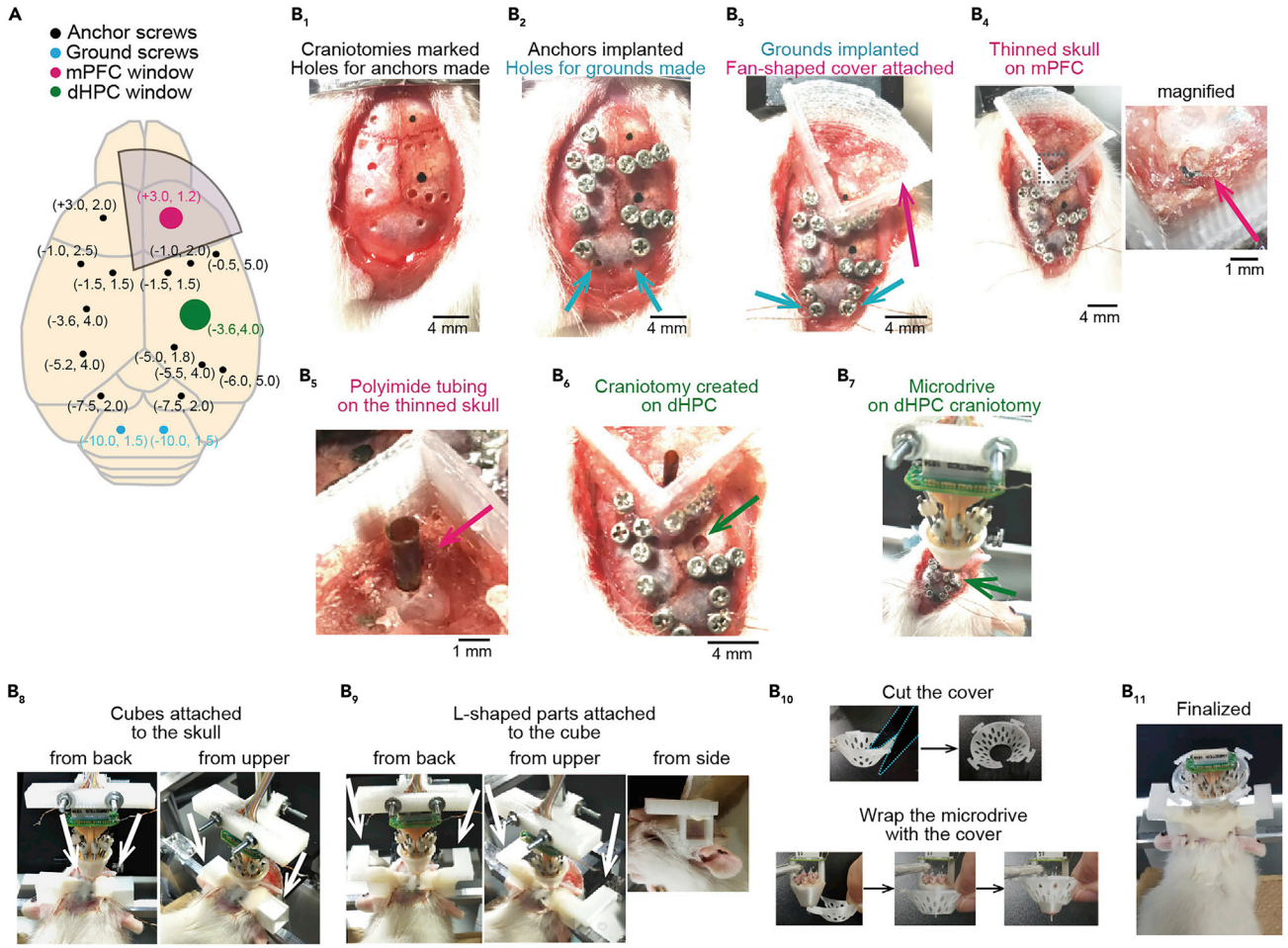

Figure 2. Surgical procedures

(A) Locations for drilling holes in the skull, viewed from the top. The values in parenthesis beside the holes represent approximate coordinates from the bregma (in mm; anterior, lateral).

(B_1–B_{11}) Critical surgical steps are shown. The cyan arrows in B_2 indicate holes for multiunit ground electrode screws. The cyan arrows in B_3 indicate holes for implanted multiunit ground electrode screws and the magenta arrow in B_3 indicates the fan-shaped cover attached to the skull. The dotted box in the left panel in B_4 is magnified in the right panel. The magenta arrow in B_4 is the thinned skull on the mPFC. The picture in B_5 is vertically flipped from that in B_4. The magenta arrow in B_5 indicates the polyimide tuning put on the thinned skull. The arrow in B_6 indicates the cranial window for the dHPC. The arrow in B_7 indicates the cranial window for the dHPC. The arrows in B_8 indicate the 1-cm cubes. The arrows in B_9 indicate the L-shaped parts attached on the cubes. Pictures in B_{10} were taken with the black background for visibility. In B_{10}, make a vertical incision throughout the cover with a scissors (cyan dots) (top) and wrap the microdrive with the cover from the bottom part of the microdrive (bottom, from left to right).

⚠ CRITICAL: A 26 gauge needle is helpful to put adhesive to small areas around the edge of the cover from both the inside and outside.

⚠ CRITICAL: Avoid putting adhesives to the skin.

9. Make a craniotomy on the skull with a diameter of 1.4 mm above the right mPFC using a high-speed drill (Figure 2B_4). Putting a small drop of 70% ethanol on the skull is helpful to soften the bone while drilling. Stop drilling when the skull becomes a thin membrane (thin skull). Leave the dura intact.

⚠ CRITICAL: Perform this step under the stereomicroscope. Using a small drill bit (e.g., 0.80 mm diameter), drill around the target point to thin the bone.

⚠ CRITICAL: Avoid penetrating the skull and exposing the dura.

10. Gently put the polyimide tubing vertically onto the thinned skull to physically protect it (Figure 2B$_5$). This process does not use any adhesives. If the tubing does not fit the thinned skull, make the diameter of thinned skull larger or make a small cut along the tubing so that the diameter of tubing is flexibly adjustable. Sterilize the surface of the thin skull, the tubing, and the fan-shaped cover with 70% ethanol, and place surgical tape (~20 mm) on the tubing to protect the thin skull from dust during subsequent housing.
11. To implant a microdrive into the dHPC, perform a craniotomy with a diameter of ~2 mm (fitted to the bundle of the microdrive) using a high-speed drill (Figure 2B$_6$).

⚠ CRITICAL: Perform this step at high magnification under the stereomicroscope. Avoid blood vessels as much as possible. Make sure to avoid drilling through the bone and dura all at once.

12. Make a small incision in the dura above the right dHPC using the tip of a 26 gauge needle. Using forceps with very fine tips, take hold of the dura at the incision and gently pull it away until the dura is removed. All layers of the dura must be removed to ensure that the tetrodes can enter into the brain cleanly. Once the dura is removed, keep the brain surface from drying out (i.e., with saline) during the rest of the procedure.

⚠ CRITICAL: Perform this step at high magnification under the stereomicroscope. Avoid blood vessels as much as possible.

troubleshooting 1

13. Position the tip of the bundle of the microdrive at a distance of ~3 cm above the craniotomy using the custom-made microdrive holder and slowly lower it using the manipulator until the tip is placed inside the skull and contacts the surface of the brain (Figure 2B$_7$).

⚠ CRITICAL: Perform this step at high magnification under the stereomicroscope.

14. Place a drop (~0.05 ml) of the sodium alginate solution using a pipette to cover the craniotomy and the tip of the bundle, and then place a drop (~0.05 ml) of the CaCl2 solution using a pipette to the same area. Mixing the two solutions yields a gel within 1 min, covering the craniotomy and the tip of the bundle. Try this step until the entire craniotomy is protected from outside air.

⚠ CRITICAL: Perform this step at high magnification under the stereomicroscope.

Note: This gel prevents the craniotomy and the bundle from attaching to the dental cement.

15. Pour liquid dental cement at a thickness of ~4.0 mm throughout the surface of the brain and wait until it turns solid. This is the first step to lightly secure all of the wires, all of the stainless-steel screws, and the bundle of the microdrive to the skull. Do not secure the patch-clamp reference ring from the multiunit ground screw electrodes. At this point, keep the microdrive by the holder.
16. Attach the 1-cm cube as an anchor to each side of the exposed skull at the location above the ear (equal to the bottom line of the dental cement put in step 15) with dental cement (Figure 2B$_8$). Then, attach a L-shaped part on the cube with dental cement on each side (Figure 2B$_9$). If the L-shaped parts are not perfectly horizontally placed, try to adjust their positions before they are completely fixed to the cube. These anchor parts are subsequently used for fixing the rat to the stereotaxic apparatus for patch-clamp recordings.

⚠ CRITICAL: Both sides of the cube and L-shaped parts must be placed horizontally. This procedure is crucial to horizontally fix the rat's head for subsequent patch-clamp recordings.

17. Cut vertically the microdrive cover with scissors (Figure 2B$_{10}$, top) and wrap the microdrive with the cover (for more detail, see Figure 2B$_{10}$, bottom).
18. Solder the open ends of the wires from the multiunit ground screw electrodes (Figure 1E) to ground channels on the electrical interface board on the microdrive.
19. Similar to step 15, secure all of the wires, the microdrive, and microdrive cover, to the skull. Leave the patch-clamp reference ring part of the multiunit ground screw electrodes protruding outside the microdrive as they are used as reference electrodes for patch-clamp recordings (step 35). Repeat this step until dental cement covers ~90% of the bundle of the microdrive and the internal sides of the 1-cm cubes. Detach the microdrive holder from the rat's head when finalized (Figure 2B$_{11}$).

⚠ CRITICAL: Make sure to fill the space on the exposed skull at the front side of the fan-shaped cover with dental cement.

20. Insert the tip of the tetrodes from the bundle at a depth of 0.75 mm into the brain by turning the screws on the microdrive.
21. Remove the rat from the stereotaxic apparatus. Terminate the anesthesia. Place the rat in a plastic cage and confirm that the animal spontaneously wakes up from anesthesia. House the rat individually. As some rats jump within a cage, use a relatively large cage with a sufficient height to prevent physical interference of the microdrive with the ceiling of the housing cage. Our cage is 29.5 cm × 45 cm in size and 26 cm in height with a hole for a water bottle nozzle on the wall. Provide food pellets on the bedding.
22. Following surgery, house the rat individually in the cage with free access to water and food for at least 7 days. Monitor the body weight every day and confirm that post-surgery body weight returns to pre-surgery body weight.

Adjustment of electrode depth, behavioral training, and habituation to a head-fixed condition

Timing: 2–4 weeks (approximately 120 min per day)

Tetrodes reach the hippocampal cell layer. The rats are fully trained for behavioral task and habituated to a head-fixed condition.

23. Beginning the day after the surgery, connect the rat to the multiunit recording equipment via the recording headstage (Figure 3A) and perform tetrode turning to advance the tetrode tips 25–250 μm per day for 2–4 weeks until spiking cells are observed from the hippocampal cell layer. Generally, one tetrode can record 3–10 hippocampal pyramidal neurons with spike amplitudes of more than 100 μV when the tetrode was properly positioned on the cell layer, as indicated by apparent clusters of neuronal spike parameters (waveform amplitudes, the peak-to-trough amplitude differences, and waveform energies) in multidimensional projection space (Buzsaki, 2004; Lin et al., 2006; Michon et al., 2016; Mou and Ji, 2018; Osanai et al., 2019; Shan et al., 2017). Once the tetrodes are adjacent to the cell layer, settle the tetrodes at those positions for stable recording over a period of several days.

Note: This procedure is similar to general protocols performed in a number of studies with tetrode recordings.

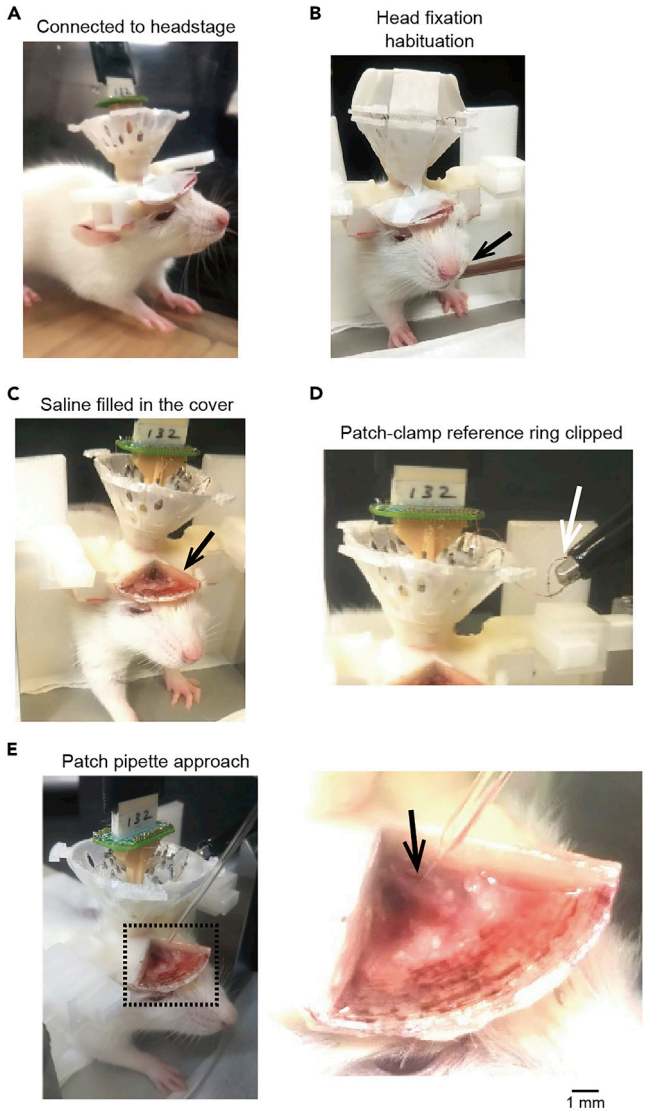

Figure 3. Critical steps after multiunit electrode implantation

The arrow in B indicates feeding of chocolate milk from the pipette. The arrow in C indicates saline solution filled in the fan-shaped cover. The arrow in D indicates the wire ring connected to the alligator clip. The dotted box in the left panel in E is magnified in the right panel. The arrow in E indicates the patch pipette tip.

24. Each day, after electrode turning, train animals on behavioral tasks (e.g., spatial task), if appropriate. Start food restriction for behavioral training at least 7 days after the surgery, if necessary. In this case, care must be taken to maintain each rat's body weight to more than 85% of its ad libitum weight.

Note: After electrode tuning and behavioral training, habituate the rat to a head fixation condition, as described in the next step.

25. Fix the rat's head to a plastic headplate (Figures 1H and 3B). Attach plastic barriers to the stereotaxic apparatus with surgical tapes (Figures 1I and 3B). This barrier physically protects the microdrive and patch pipettes from scratching by the hindlimbs.
26. To habituate the rat to the head fixation condition, provide a chocolate milk drop directly to the rat's mouth using a pipette for 10–30 min. On the first five days, keep a pipette delivering the

chocolate milk solution to the rat's mouth throughout the habituation period for up to 10 min. Terminate this daily habituation when the rat begins to exhibit substantial movement. When the rat becomes familiar with this condition after five days of habituation, increase the habituation duration to 30 min by providing a chocolate milk drop (~0.3 ml) every 5 min using a pipette. When the rat moves the hindlimb, provide chocolate milk immediately. This habituation lasts 10–17 days.

⚠ CRITICAL: Some rats continuously move substantially (e.g., kicking and crying) during head fixation. This issue sometimes happens even one week after habituation. If the rat continues to show intense movement for three consecutive days, terminate the experiment and euthanize the rat, as it is impossible to obtain patch-clamp recordings from such rats. To our experience, 7 out of 51 (13.7%) rats showed such behavior and the experiments were terminated before patch-clamp recordings.

Multiunit recordings of dHPC neurons during a behavioral period

Timing: 60 min (flexible)

Spike patterns are recorded from dHPC neuronal ensembles during behavioral tasks.

27. Perform multiunit data recordings from the dHPC during a behavioral task once the rat has sufficiently learned the task and well-separated unit activity is identified in the dHPC (Buzsaki, 2004; Michon et al., 2016; Mou and Ji, 2018; Osanai et al., 2019).

Note: This is a general step for multiunit recordings. In our recording, the sampling rate of LFP signals is 2 kHz, and unit spike waveforms are bandpass filtered at 600 Hz to 6 kHz and recorded at 30 kHz for 1.6 ms when the amplitude exceeds a trigger threshold. Monitor the rat's behavior using a video camera, if appropriate.

Patch-clamp recordings

Timing: 60 min

After the rat is head-fixed, membrane potential changes are recorded from mPFC neurons by whole-cell recordings.

28. After the multiunit recordings from the freely moving rat are finished, fix the rat to the stereotaxic apparatus and attach plastic barriers to the stereotaxic apparatus, similar to the habituation step (step 25).
29. Cut the whiskers to prevent contact with the patch pipettes.
30. Apply ~1 ml of 0.5% lidocaine solution dissolved in saline as an analgesic to the saline pool surrounded by the fan-shaped cover above the skull of the mPFC (Figure 3C).

⚠ CRITICAL: This analgesic is necessary for the next step 31.

31. Remove the polyimide tubing from the thin skull above the mPFC.

⚠ CRITICAL: Do not use a drill, as the rat is awake.

⚠ CRITICAL: If the surgical procedures (steps 8-10) have been correctly performed, a scab-like structure is generally formed on the thin skull in the lumen of the polyimide tubing. When the tube is removed from the head, the scab-like structure and the thin skull should be easily peeled off together.

troubleshooting 2 and 3

32. Remove the lidocaine solution in the pool by a pipette and apply the same amount of saline to the pool.
33. Make a small incision in the dura above the mPFC using a 30-gauge stainless-steel needle. Using forceps with very fine tips, take hold of the dura at the incision and gently pull it away until the dura is removed. All layers of the dura must be removed to ensure that patch pipettes can enter the brain cleanly. Once the dura is removed, keep the brain surface from drying out (i.e., with saline) during the rest of the procedure.

⚠ CRITICAL: Perform this step at high magnification under the stereomicroscope.

⚠ CRITICAL: Perform this step carefully to minimize damage to the brain tissue and bleeding around the dura.

troubleshooting 4

34. Dip a patch-clamp ground electrode (generally, it is a stone-shaped electrode protruding from the headstage of the patch-clamp recording system) in the saline pool, serving as a ground electrode for patch-clamp recordings.
35. Connect alligator clips to the patch-clamp reference ring part of the multiunit ground screw electrodes protruding outside the microdrive (step 19) (Figure 3D). Then, connect the other end of the clip to any metal parts of the patch-clamp ground electrode.

Note: This step is necessary in multiunit recordings to cancel electrical noise arising from the patch-clamp recording setup.

36. Through the hole, lower a borosilicate glass pipette filled with whole-cell internal solution, tilted at an angle of 10–15° to the posterior side and 0–15° to the medial or lateral side, to the mPFC at a depth of 750–3600 μm from the cortical surface (Figure 3E). First, lower the pipette relatively faster at a speed of 50–100 μm/s before reaching an approximate target depth. Then, reduce the speed to 1–2 μm/s to access a neuron to obtain a patch-clamp recording. This final process of accessing a patch pipette to a neuron in the brain is similar to the protocols used for *in vivo* patch-clamp recordings (Lee et al., 2009; Lee et al., 2014; Petersen, 2017). Apply rectangular current pulses continuously during access and monitor changes in voltage responses to the pulses.

⚠ CRITICAL: Perform this step while the rat does not show bruxism, which disturbs the monitoring of the correct voltage responses.

⚠ CRITICAL: Perform this step in a silent environment. Loud sounds stimulate movement by the rat, which reduces the success rates of patch-clamp recordings.

⚠ CRITICAL: The angle of access of the patch pipette needs to be flexibly adjusted to prevent physical interference between the patch pipette and the microdrive.

troubleshooting 5

37. Obtain whole-cell recordings from a neuron by recording equipment using standard *in vivo* whole-cell recording methods (Lee et al., 2009; Lee et al., 2014; Petersen, 2017). Generally, it should require approximately 10–20 attempts to obtain a stable whole-cell recording in one rat.

⚠ CRITICAL: Discard neurons when the series resistance exceeds 75 MOhm or the mean resting potential exceeds –50 mV. Truncate recordings when the spike peak decreases below –10 mV or the resting potential increases by more than 40 mV from its baseline value at the onset of the recording. Null the liquid junction potential offline.

troubleshooting 6

38. If patch-clamp recordings are not successful, it is possible to try again within the next 2 days before thick tissue is formed on the mPFC craniotomy. In that case, place polyimide tubing on the craniotomy to protect the craniotomy again, as described in step 10.
39. At the beginning of each whole-cell recording, inject depolarizing and hyperpolarizing 1000-ms rectangular currents from –200 to +350 pA into the cell at steps of 50 pA to characterize the cell's intrinsic properties and spike responses. Select cells that show typical regular-spiking characteristics as principal cells.
40. Throughout this recording process, confirm that the rat exhibits no behavioral signs of pain.

Histological verification of recording locations

Timing: 3 days

Recording locations of tetrodes and cell morphology of the patched neurons are verified in the dHPC and mPFC, respectively.

41. At the end of the patch-clamp recordings, slowly raise the patch pipette at a speed of 5 μm/s while monitoring the membrane resistance. This step is crucial to reconstruct the cell morphology without disrupting the cell membrane. First, the resistance becomes more than 1 GΩ, a sign of outside-out recording. When the resistance then becomes less than 1 GΩ, indicating that the pipette is detached from the cell membrane, increase the speed to 100 μm/s and pull the pipette out from the brain.
42. Detach the headstage of the microdrive from the rat. Inject 0.3 ml of 0.1 g/ml urethane (i.p) and wait until the rat is fully anesthetized.
43. Perfuse the brain transcardially with saline followed by a 4% PFA solution using a standard perfusion method.
44. Decapitate the rat and store the brain in air for 12 h at 4°C without withdrawing the tetrodes from the brain.

Note: This step is necessary to facilitate the reconstruction of the tetrode tracks.

45. Remove the brain and store it for 12 h at 4°C in a 4% PFA solution.
46. With a blade, coronally cut the forebrain into two pieces of tissue at approximately 6.0 mm posterior to the olfactory bulb (Figure 4A), an anterior piece containing the mPFC (tissue 1) and the remaining posterior piece containing the dHPC (tissue 2).
47. For tissue 1, slice the tissue at a thickness of 100–150 μm in PBS using a vibratome (Figure 4B).
48. To visualize the biocytin-filled cell morphology of the patched cells in the mPFC, process the slices with 2 μg/ml streptavidin-Alexa Fluor 594 conjugate and 0.2% Triton X-100 for 6 h.
49. Incubate the slices with 0.4% NeuroTrace 435/455 blue fluorescent Nissl Stain dissolved in PBS for 12 h at 4°C.
50. For tissue 2, equilibrate the tissue with a sequence of 20% sucrose in PBS for 24 h and 30% sucrose in PBS for 24 h.
51. Freeze and slice the tissue at a thickness of 150 μm using a microtome (Figure 4B).
52. Mount the slices on a coverglass and process them for a standard cresyl violet staining method. Confirm the tracks of all tetrodes in the dHPC in the histological tissue.

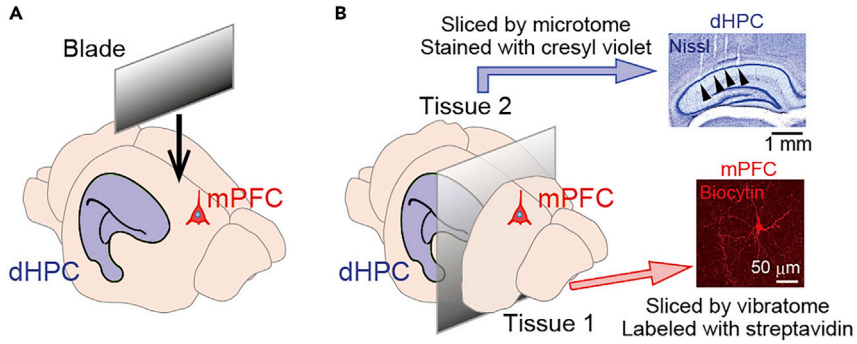

Figure 4. Procedures for histological verification

(A) The forebrain is divided into two pieces of tissue with a blade, an anterior part containing the mPFC (tissue 1) and a posterior part containing the dHPC (tissue 2).

(B) (Left) Slices from tissue 1 are stained with streptavidin, whereas slices from tissue 2 are stained with cresyl violet. (Right) Representative images of a cresyl violet-stained brain section showing tetrode locations in the dHPC (top, black arrowheads) and a biocytin-labeled patched mPFC neuron (bottom).

EXPECTED OUTCOMES

Here we introduced a protocol to simultaneously record the spike activity patterns of a dHPC neuronal population and membrane potential of an mPFC neuron from an awake rat. When following our protocol, individuals who are fully familiar with both recording techniques will succeed in the concurrent recordings by approximately 5 training experiments (rats). For trained experimenters, the success rate of dHPC multiunit recordings (until step 27) is almost 100% but the number of simultaneously recorded dHPC neurons considerably varies, ranging from 0 to 30 neurons, depending on the quality of daily tetrode turning processes (step 23). After that, the success rate of concurrent multiunit and patch-clamp recordings from one rat is approximately 50% based on the fact that the success rate of each attempt to obtain a whole-cell recording from a mPFC neuron is 5% and the number of attempts allowed in one rat is 10–20 times. The patch-clamp recordings are stable for up to 20 min (on average, 10 min). If one maintains a good condition in which the rat keeps silent and few attempts were made before obtaining a patch-clamp recording, it is possible to try another recording from a different mPFC neuron at a different coordinate within the craniotomy (in this case, a different coordinate should be selected to distinguish from the former patched neuron). We indeed recorded two mPFC neurons from a single rat (n = 3 rats). The success of morphological reconstruction of patched neurons depends on whether one can start retracting a pathed pipette (step 41) before the occurrence of prominent depolarization, a sign of disruption, during a whole-cell recording. If this step is properly performed, the success rate of reconstruction is almost 100%. Overall, over the past 2 years, experienced experimenters have been able to obtain approximately 20 successful recordings. All protocols can be performed by one person, or some steps may be shared by several persons (e.g., surgery for the implantation of electrodes and covers, turning, habituation, and patch-clamp recordings).

Typical recording data are shown in Figure 5B. Here, the rat first performed a spatial task in which it ran back and forth on a U track to obtain a chocolate milk reward placed at the track end for 10 min (behavior). During this task, some dHPC cells exhibited place-selective firing, represented as place cells. Then, the rat was head-fixed, and a whole-cell recording was obtained from an mPFC neuron while the same dHPC neurons were recorded (head fixation). During this post-task period, some dHPC neurons were synchronously reactivated, which potentially represented memory consolidation mechanisms (Eschenko et al., 2008; Kudrimoti et al., 1999). Figure 5C shows example datasets illustrating how individual synchronization events of the dHPC neurons (defined at a time window of 100 ms) are associated with changes in the subthreshold potentials (ΔV_m) of the mPFC neuron. These traces are converted to the distributions of the amplitude of mPFC ΔV_m (computed at a post-event time window of 0–150-ms) constructed for different numbers (2, black; 3, cyan; 4, magenta) of dHPC

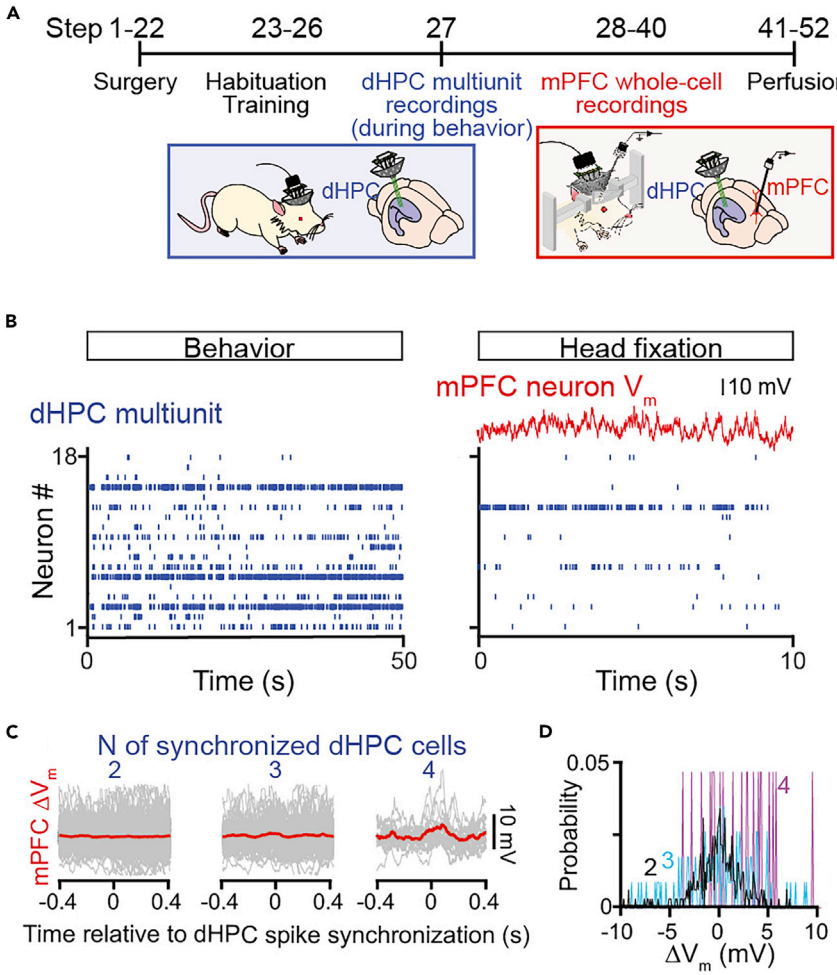

Figure 5. Simultaneous multiunit recordings from dHPC neurons and a whole-cell recording from an mPFC neuron

(A) The experimental timeline. After spike patterns of dHPC neurons are recorded from a freely behaving rat, the rat was fixed on a stereotaxic apparatus, and whole-cell recording is performed on an mPFC neuron while the corresponding dHPC neurons are continuously recorded.

(B) (Left) Spike patterns of dHPC neurons during behavior. Each row represents a dHPC neuron, and each dot represents a spike. (Right) Spike patterns of identical dHPC neurons (blue) and membrane voltage of a mPFC neuron (red) during head fixation.

(C) From left to right, changes in membrane voltage traces of the mPFC neuron aligned to the time of synchronous firing of 2, 3, and 4 dHPC neurons (gray, individual traces; red, average).

(D) The probability distributions of membrane voltage changes in the mPFC neuron at the individual dHPC synchronization. The values show the numbers of synchronized neurons (black, 2; cyan, 3; magenta, 4).

synchronized cells (Figure 5D). In this neuron, the mPFC ΔV_m at 4 dHPC synchronized cells was significantly higher than the values at 2 and 3 dHPC synchronized cells (2 vs 3, $Z = 1.95$, $P = 0.10$; 2 vs 4, $Z = 2.25$, $P = 0.049$; Mann-Whitney U test followed by Bonferroni correction). More detailed analyses for these datasets have been described in (Nishimura et al., 2021). These results suggest that larger spike synchronization of dHPC neurons leads to stronger depolarization in mPFC neurons, implicating a mechanism by which mPFC neurons can preferentially read out organized activity patterns arising from the dHPC (Jadhav et al., 2016; Shin et al., 2019; Tang et al., 2017).

A similar circuit mechanism may work in other brain areas as a principle of activity-dependent information transfer across neuronal ensembles. This experimental technique provides a unique means to directly address these issues by simultaneously obtaining multiunit spike patterns of neurons in

one brain region and membrane potentials of a neuron in the other region. Accumulation of these insights will bridge long-standing gaps between extracellularly recorded neuronal population spikes at suprathreshold levels related to brain functions and intracellularly recorded synaptic transmission underlying these spike patterns at subthreshold levels, both of which have long been studied independently.

LIMITATIONS

This protocol is not applicable to a pair of brain regions that are too close to each other (<5 mm) on the horizontal plane of the brain surface due to physical interference between the microdrive and the patch-clamp pipette. The samples need to be discarded if the rats are not sufficiently habituated or sufficient whole-cell recordings are not obtained. The morphology of patched neurons may not be reconstructed if whole-cell recordings are accidentally terminated due to excess physical movement or cell membrane disruption, while a good reconstruction result can be expected if a pathed pipette is retracted after a >3-min recording without such disruption. Sudden disruption of a whole-cell recording within 3 min generally results in the poor quality of reconstruction (e.g., only soma visualized or too low fluorescent intensity), due to insufficient fills of biocytin. A duration to maintain a good patch-clamp recording condition is limited within 20 min.

TROUBLESHOOTING

Problem 1

Bleeding does not stop after removing the dura (step 12).

Potential solution

Hemostasis is not sufficient. Repeatedly wash the brain surface with fresh saline and position absorbent gauze and a gel form to remove blood. This procedure takes up to 30 min.

Problem 2

Brain edema occurs around the craniotomy on the mPFC (step 31).

Potential solution

The skull is penetrated by drilling (step 9), and the dura is exposed for several weeks. Carefully perform step 9. Do not penetrate the skull when drilling. Sterilize the polyimide tubing and the surface of the skull.

Problem 3

Thick tissue is formed on the thin skull (step 31).

Potential solution

Surgical procedures (steps 9 and 10) are not performed properly. Carefully perform step 9. Do not penetrate the skull when drilling. Sterilize the polyimide tubing and the surface of the skull.

Problem 4

Multiunit signals from the HPC are lost when removing the dura (step 33).

Potential solution

The brain is moved when removing the dura. Gently and slowly perform this step to establish a durectomy.

Problem 5

Bleeding makes accessing patch pipettes difficult (step 36).

Potential solution

Avoid blood vessels as much as possible. Repeatedly wash the brain surface with fresh saline and position absorbent gauze and a gel form to remove blood.

Problem 6

Whole-cell recordings are not obtained or are lost immediately (step 37).

Potential solution

Increase the habituation time so that the rat is stabilized. Tightly secure all devices and fix the rat to the stereotaxic apparatus. Use shorter pipettes. For more details of general *in vivo* patch-clamp procedures, see (Lee et al., 2009; Lee et al., 2014; Petersen, 2017).

RESOURCE AVAILABILITY

Lead contact

Further information and requests for resources and reagents should be directed to and will be fulfilled by the lead contact, Takuya Sasaki (tsasaki@mol.f.u-tokyo.ac.jp).

Materials availability

All the CAD files used in this paper are available at Mendeley Data (https://data.mendeley.com/datasets/4szrgxvm37/1).

Data and code availability

The datasets generated during this study are available at Mendeley Data (https://dx.doi.org/10.17632/kc49ctr6yb.1).

ACKNOWLEDGMENTS

This work was supported by KAKENHI (19H04897; 20H03545; 21H00185) from the Japan Society for the Promotion of Science (JSPS), a Precursory Research for Embryonic Science and Technology grant (JPMJPR1785) from the Japan Science and Technology Agency (JST), and a grant from the Advanced Research & Development Programs for Medical Innovation (1041630) of the Japan Agency for Medical Research and Development (AMED) to T.S.; funds from the JST Exploratory Research for Advanced Technology (JPMJER1801) and the AMED Strategic International Brain Science Research Promotion Program (18dm0307007h0001) to Y.I.; and a JSPS Research Fellowship for Young Scientists to Y.N.

AUTHOR CONTRIBUTIONS

Conceptualization, Y.N. and T.S.; investigation, Y.N. and T.S.; writing – original draft, Y.N. and T.S.; writing – review & editing, Y.N., Y.I., and T.S.; funding acquisition, Y.N., Y.I., and T.S.; supervision, Y.I. and T.S.

DECLARATION OF INTERESTS

The authors declare no competing interests.

REFERENCES

Bittner, K.C., Grienberger, C., Vaidya, S.P., Milstein, A.D., Macklin, J.J., Suh, J., Tonegawa, S., and Magee, J.C. (2015). Conjunctive input processing drives feature selectivity in hippocampal CA1 neurons. Nat. Neurosci. *18*, 1133–1142.

Buzsaki, G. (2004). Large-scale recording of neuronal ensembles. Nat. Neurosci. *7*, 446–451.

Davison, I.G., and Ehlers, M.D. (2011). Neural circuit mechanisms for pattern detection and feature combination in olfactory cortex. Neuron *70*, 82–94.

Ebbesen, C.L., Doron, G., Lenschow, C., and Brecht, M. (2017). Vibrissa motor cortex activity suppresses contralateral whisking behavior. Nat. Neurosci. *20*, 82–89.

Epsztein, J., Lee, A.K., Chorev, E., and Brecht, M. (2010). Impact of spikelets on hippocampal CA1 pyramidal cell activity during spatial exploration. Science *327*, 474–477.

Eschenko, O., Ramadan, W., Molle, M., Born, J., and Sara, S.J. (2008). Sustained increase in hippocampal sharp-wave ripple activity during slow-wave sleep after learning. Learn. Memory *15*, 222–228.

Harvey, C.D., Collman, F., Dombeck, D.A., and Tank, D.W. (2009). Intracellular dynamics of hippocampal place cells during virtual navigation. Nature *461*, 941–946.

Inagaki, H.K., Fontolan, L., Romani, S., and Svoboda, K. (2019). Discrete attractor dynamics

underlies persistent activity in the frontal cortex. Nature *566*, 212–217.

Jadhav, S.P., Rothschild, G., Roumis, D.K., and Frank, L.M. (2016). Coordinated excitation and inhibition of prefrontal ensembles during awake hippocampal sharp-wave ripple events. Neuron *90*, 113–127.

Jog, M.S., Connolly, C.I., Kubota, Y., Iyengar, D.R., Garrido, L., Harlan, R., and Graybiel, A.M. (2002). Tetrode technology: advances in implantable hardware, neuroimaging, and data analysis techniques. J Neurosci. Methods *117*, 141–152.

Kloosterman, F., Davidson, T.J., Gomperts, S.N., Layton, S.P., Hale, G., Nguyen, D.P., and Wilson, M.A. (2009). Micro-drive array for chronic in vivo recording: drive fabrication. J. Vis. Exp. 1094.

Kudrimoti, H.S., Barnes, C.A., and McNaughton, B.L. (1999). Reactivation of hippocampal cell assemblies: effects of behavioral state, experience, and EEG dynamics. J. Neurosci. *19*, 4090–4101.

Lee, A.K., Epsztein, J., and Brecht, M. (2009). Head-anchored whole-cell recordings in freely moving rats. Nat. Protocol. *4*, 385–392.

Lee, D., Lin, B.J., and Lee, A.K. (2012). Hippocampal place fields emerge upon single-cell manipulation of excitability during behavior. Science *337*, 849–853.

Lee, D., Shtengel, G., Osborne, J.E., and Lee, A.K. (2014). Anesthetized- and awake-patched whole-cell recordings in freely moving rats using UV-cured collar-based electrode stabilization. Nat. Protocol. *9*, 2784–2795.

Lin, L., Chen, G., Xie, K., Zaia, K.A., Zhang, S., and Tsien, J.Z. (2006). Large-scale neural ensemble recording in the brains of freely behaving mice. J. Neurosci. Methods *155*, 28–38.

Margrie, T.W., Meyer, A.H., Caputi, A., Monyer, H., Hasan, M.T., Schaefer, A.T., Denk, W., and Brecht, M. (2003). Targeted whole-cell recordings in the mammalian brain in vivo. Neuron *39*, 911–918.

Michon, F., Aarts, A., Holzhammer, T., Ruther, P., Borghs, G., McNaughton, B., and Kloosterman, F. (2016). Integration of silicon-based neural probes and micro-drive arrays for chronic recording of large populations of neurons in behaving animals. J. Neural. Eng. *13*, 046018.

Mou, X., and Ji, D. (2018). Large-scale tetrode recording in the rodent hippocampus. In Extracellular Recording Approaches, R.V. Sillitoe, ed. (Springer New York), pp. 87–107.

Nelson, S., Toth, L., Sheth, B., and Sur, M. (1994). Orientation selectivity of cortical neurons during intracellular blockade of inhibition. Science *265*, 774–777.

Nguyen, D.P., Layton, S.P., Hale, G., Gomperts, S.N., Davidson, T.J., Kloosterman, F., and Wilson, M.A. (2009). Micro-drive array for chronic in vivo recording: tetrode assembly. J. Vis. Exp. 1098.

Nishimura, Y., Ikegaya, Y., and Sasaki, T. (2021). Prefrontal synaptic activation during hippocampal memory reactivation. Cell Rep. *34*, 108885.

Osanai, H., Kitamura, T., and Yamamoto, J. (2019). Hybrid microdrive system with recoverable opto-silicon probe and tetrode for dual-site high density recording in freely moving mice. J. Vis. Exp.

Pei, X., Volgushev, M., Vidyasagar, T.R., and Creutzfeldt, O.D. (1991). Whole cell recording and conductance measurements in cat visual cortex in-vivo. Neuroreport *2*, 485–488.

Petersen, C.C.H. (2017). Whole-cell recording of neuronal membrane potential during behavior. Neuron *95*, 1266–1281.

Poo, C., and Isaacson, J.S. (2011). A major role for intracortical circuits in the strength and tuning of odor-evoked excitation in olfactory cortex. Neuron *72*, 41–48.

Poulet, J.F., and Petersen, C.C. (2008). Internal brain state regulates membrane potential synchrony in barrel cortex of behaving mice. Nature *454*, 881–885.

Shan, K.Q., Lubenov, E.V., and Siapas, A.G. (2017). Model-based spike sorting with a mixture of drifting t-distributions. J. Neurosci. Methods *288*, 82–98.

Shin, J.D., Tang, W., and Jadhav, S.P. (2019). Dynamics of awake hippocampal-prefrontal replay for spatial learning and memory-guided decision making. Neuron *104*, 1110–1125.e7.

Tang, W., Shin, J.D., Frank, L.M., and Jadhav, S.P. (2017). Hippocampal-prefrontal reactivation during learning is stronger in awake compared with sleep states. J. Neurosci. *37*, 11789–11805.